Design Review: A Low-Cost Mini Bipedal Robot

Vincent Trosky, Nelson Rosa
Mechanical, Material, and Aerospace Engineering Department
Illinois Institute of Technology
Chicago, IL, United States

***Abstract*—This paper examines the design process and alpha prototype of a low-cost mini bipedal robot. Testing control algorithms for bipedal robots on physical hardware can become a time-consuming and expensive process. The robot presented in this paper offers a modular, open-source platform for bipedal control algorithm testing for roughly $200. The manufacturing process requires simple 3D-printing, turning, and drilling operations. The final prototype can stand passively and will soon be tested using a planar support mechanism on a treadmill to constrain the robot to the saggital plane and identify compatible control approaches.**

I. Introduction

Bipedal robots have become increasingly popular both in the research and private spheres of engineering development. Their growing prevalence can be attributed to recent advances in hardware, control approaches, and an explosion of multi-billion dollar investment into humanoid development. While many of these robots are very complex, with upwards of 30+ degrees of freedom (DOF), their control algorithms use simplified models to represent their physical body and reduce computational complexity [1] [2] [3]. The prototype in this paper is based off of the Spring-loaded Inverted Pendulum (SLIP) and SLIP with Swing Leg (SLIP-SL) models. When attached to the planarizing mechanism, the robot is fully actuated, maintaining four DOF which are controlled using four different actuators (see Fig. 1).

This paper outlines the design process and final result of the mini bipedal prototype as follows: Section II describes the mathematical models that inspired the robot design, Section III describes the prototype design and manufacturing process, and Section IV outlines future plans for this project.

II. Mathematical Modeling of Bipedal Robots

This section will review two publications that outline mathematical models which are applicable to the design presented in this paper. The models explored in this section include the SLIP and SLIP-SL models which are each passive models that can be adapted to accept the proper control inputs.

A. Robust and Efficient Walking With Spring-like Legs

This paper [4] outlines a "bipedal spring-mass model", otherwise known as the Spring-Loaded Inverted Pendulum (SLIP) model. This model is widely used throughout bipedal research literature as a basis for designing bipedal robots. The model assumes that each leg is mass-less and that the robot's entire mass can be interpreted as a point mass m near the hip at $\mathbf{r} = [x, y]^T$. As seen in Fig. 2, the SLIP model has two primary phases: single support and double support. In the single support case, the system dynamics remain unaffected by the mass-less swinging leg. Each leg is compliant, starting at length L_0 and compressing via Hooke's law to length L according to spring constant k. Forces $\mathbf{F}$ are applied by the legs from foot point $\mathbf{r_{FP}}$ onto $\mathbf{r}$. The equation of motion is represented in the 2-D plane

$$m\ddot{\mathbf{r}} = \mathbf{F}_1 + \mathbf{F}_2 + m\mathbf{g} \tag{1}$$

with the gravitational acceleration $\mathbf{g} = [0, g]^T$ and $g = -9.81\,\mathrm{m/s^{-2}}$. The force of leg 1 is represented as

$$F_1 = k(\frac{L_0}{|\mathbf{r} - \mathbf{r}_{FP1}|})(\mathbf{r} - \mathbf{r}_{FP1}). \tag{2}$$

This equation can be generalized for leg 2 when it is in contact with the ground. Other important variables to note

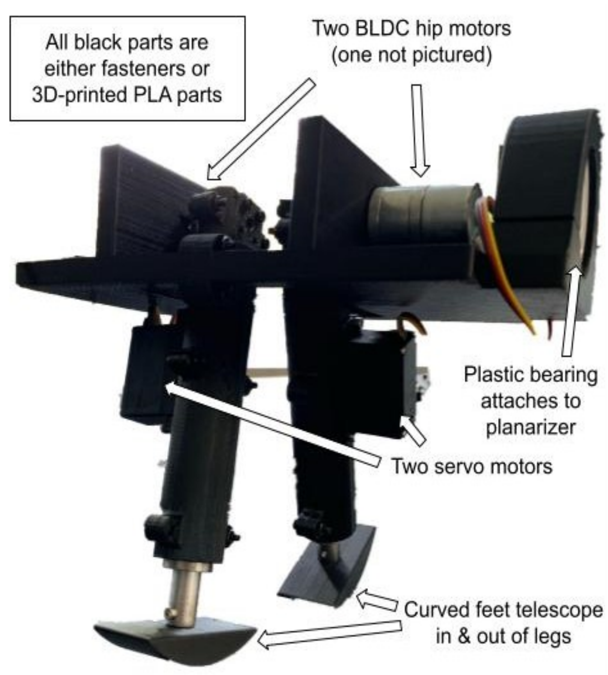

Fig. 1. Image of the final prototype, made primarily from 3D-printed materials.

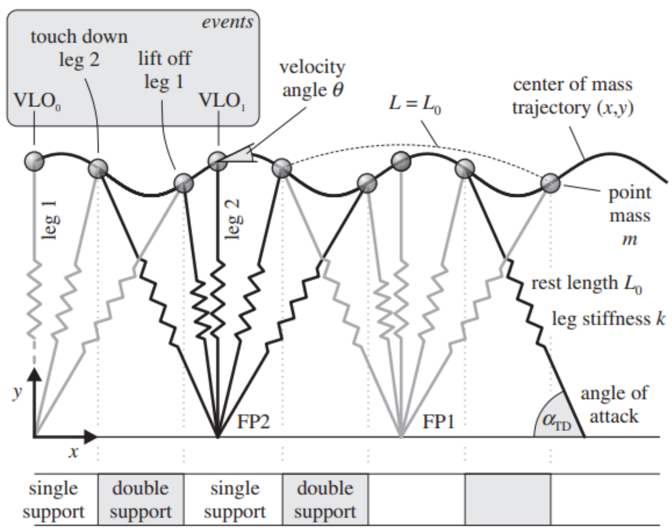

Fig. 2. SLIP Model [4]

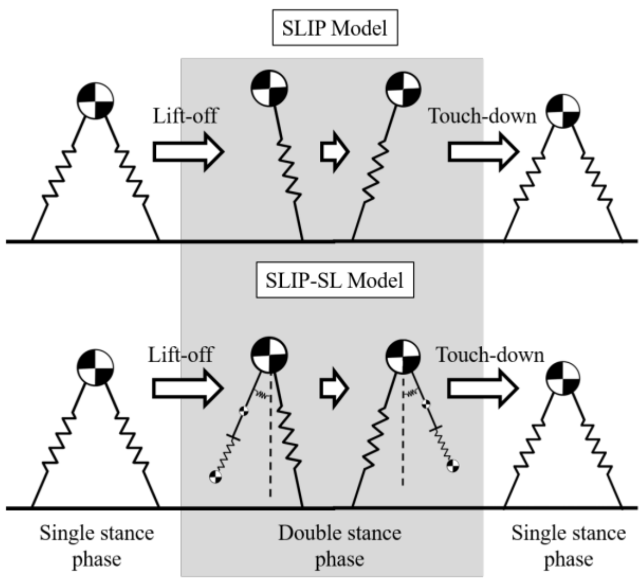

Fig. 3. SLIP Model vs SLIP-SL Model [5]

include vertical leg orientation $\mathbf{VLO}$, angle of attack α_{TD}, and velocity angle θ.

B. Bipedal Walking Based on Improved Spring Loaded Inverted Pendulum Model with Swing Leg (SLIP-SL)

This paper [5] expands on the SLIP model to develop the Spring Loaded Inverted Pendulum with Swing Leg (SLIP-SL) model. As seen in Fig. 3, the key difference is that the swing leg is no longer considered mass-less during the single support phase. The dynamics of the model in the single support phase can be written as

$$\mathbf{M}(\mathbf{q})\ddot{\mathbf{q}} + \mathbf{C}(\mathbf{q}, \dot{\mathbf{q}})\dot{\mathbf{q}} + \mathbf{G}(\mathbf{q}) = \mathbf{u}, \tag{3}$$

where $\mathbf{q} = [\theta_1, \theta_2, \theta_3]^T$ are the generalized coordinates, $\mathbf{M}(\mathbf{q}) \in R^{3\times3}$ is an inertia matrix, $\mathbf{C}(\mathbf{q}, \dot{\mathbf{q}}) \in R^{3\times3}$ is a Coriolis and centrifugal terms matrix, $\mathbf{G}(\mathbf{q}) \in R^3$ is the gravity term, and $\mathbf{u} \in R^3$ are the input torques. While in double support phase, the dynamics of the SLIP-SL model match that of the SLIP model.

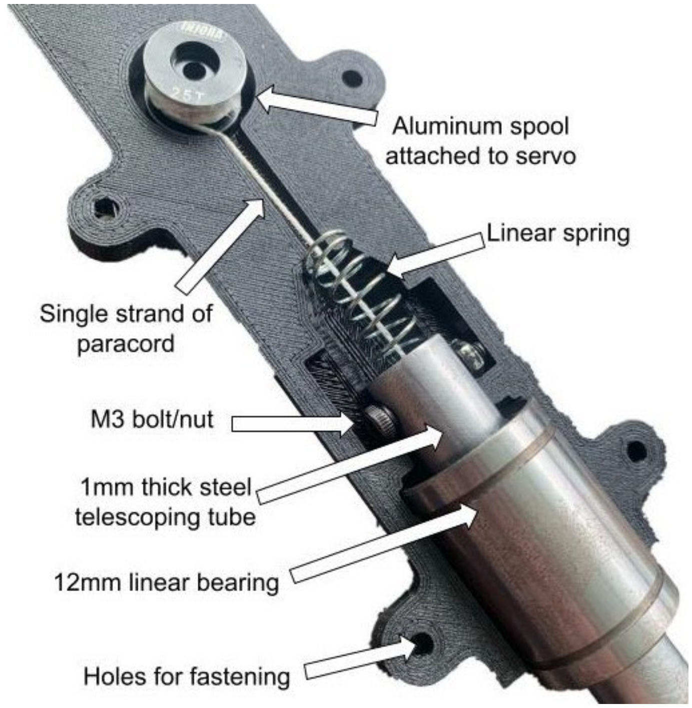

Fig. 4. A cross-sectional view of the spring-based telescoping leg mechanism. As the spool rotates, the spring is compressed and the steel tube telescopes through the linear bearing.

III. Prototype Design and Manufacturing

The design selection process for this project was motivated primarily to model the SLIP and SLIP-SL models as closely as possible. Important design considerations included minimizing mass wherever possible and utilizing cheap, modular parts.

A. Prototype Design

The final prototype has a 3D-printed hip at which two BLDC motors are mounted. The rotors of each motor are attached to each 3D-printed leg using aluminum couplings. Mounted to the leg is a Hitec HS-425BB 180° servo motor with a max torque of 320 mNm. A servo winch spool is attached to the servo, winding a single strand of paracord (see Fig. 4). Paracord is made up of many individual strands, which can easily be cut out of the sleeve that covers them. These strings were chosen due to their low elasticity and high tensile strength. The string is tied at the other end to an M3 bolt which is pinned through a 1mm steel tube. Steel was chosen for its hardness over aluminum and plastic to prevent grooves from developing on the tube's surface from the linear bearing balls. When the servo actuates, the string effectively pulls the bolt steel tube toward the spool.

When the spool is actuated in the opposite direction, the tension is released on the string, and a linear spring

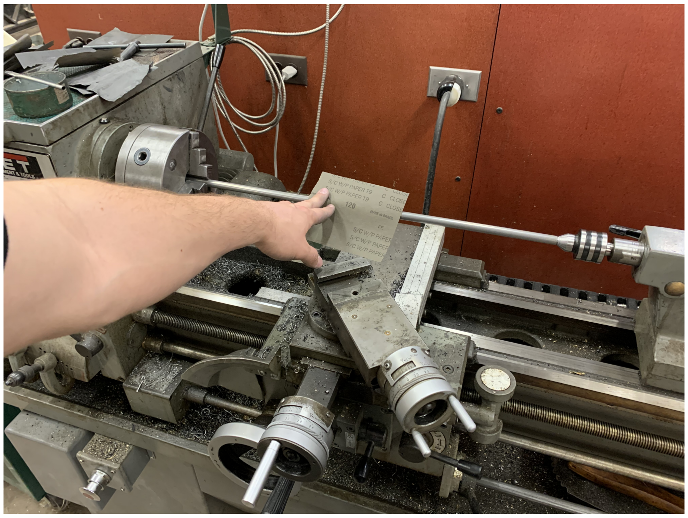

Fig. 5. Sanding tubes for the robot and planarizer down with 120-grit sandpaper.

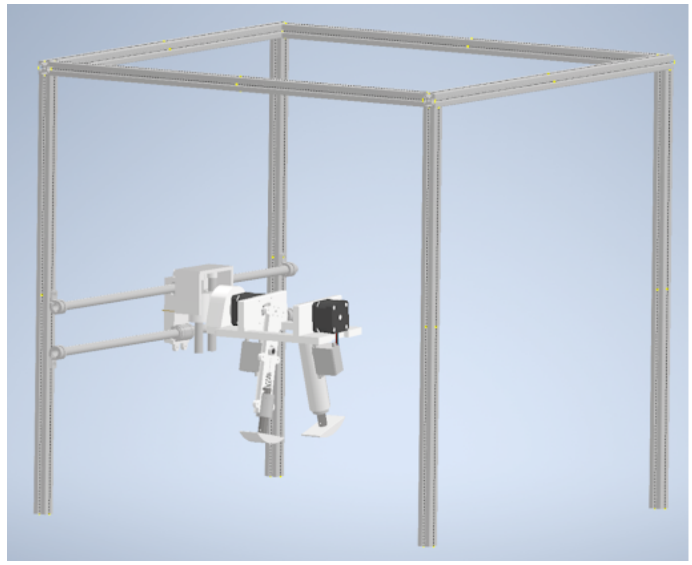

Fig. 6. The robot attached to the planarizer.

pushes the tube and foot away from the spool. The bolt sits in a channel within the leg that prevents the tube and foot from twisting while walking. However, this issue is unlikely to occur at low speed gaits due to the robot's foot shape. The foot is a 3D arc which naturally readjusts minor misalignments upon heel strike. The arc also mimics Tad McGeer's curved foot walker which used a radius of approximately 1/3 the length from the bottom of the foot to the hip [5]. This ratio was found to be the most stable out of leg lengths tested according to McGeer. This design closely mimics the SLIP and SLIP-SL model.

The design also features a modular design, allowing the user to assemble different versions of the robot. For instance, suppose the user wants to use a spring with a different spring constant, leg length, foot shape, and servo motor. With only a few CAD edits, new legs and feet can be printed in less than a day, and a spring with identical dimensions and a higher spring constant can be swapped out. Ultimately, the modular design and low price point allow users to quickly modify the baseline design and test their variations at a small cost.

B. Manufacturing Process

Wherever possible, manufacturing processes were reserved for a 3D-printer. An Ender 3 Pro printer was used with 10% infill to minimize the weight of the 3D-printed structural components. Finding proper tolerances and clearances for this robot required frequent and time-consuming trial and error. The steel tubes were cut to their proper lengths from stock and holes were drilled at the ends using a mill. The mill was used to ensure the holes were drilled in place, but a drill could also be used. To account for any misalignment in the case that a drill is used, the depths of the channels inside the 3D-printed leg could be adjusted slightly. The outer walls of each spool were also turned from 16 mm to 13 mm to shrink the spool profiles to fit in the 3D-printed legs, but this is not entirely necessary as the legs can be adjusted and reprinted.

One unforeseen issue was that the steel tubes were slightly too wide in outer diameter to slide smoothly through the linear bearings. To address this, all of the steel tubes were placed on a lathe and sanded down using 120-grit sandpaper (see Fig. 5). In future, it would likely be better to just run a finishing turning passes on the steel tubes until the correct tolerance is achieved rather than spending time hand-sanding.

IV. Toward a Stable Gait

To achieve a stable gait, the robot will need to first be mounted to its planarizer via a plastic bearing inside the hip to constrain its motion to the saggital plane (see Fig. 6). A treadmill will be paired with the planarizer. All electronics will be off-boarded until a control algorithm and mechanical design pairing achieve a stable gait. Early control algorithms will include PID-controllers, but new control algorithms will be tested until a stable gait is achieved. Further, new mechanical designs will be proposed, including designs with a backdriveable actuator and mechanical design solution that replaces the current spring and string mechanism. This will allow for more complex gait solutions, like running and hopping.

References

[1] Blickhan R. The spring-mass model for running and hopping. J Biomech. 1989;22(11-12):1217-27. doi: 10.1016/0021-9290(89)90224-8. PMID: 2625422.

[2] Mark W. Spong, Passivity based control of the compass gait biped, IFAC Proceedings Volumes, Volume 32, Issue 2, 1999, Pages 506-510, ISSN 1474-6670, https://doi.org/10.1016/S1474-6670(17)56086-3.

[3] S. Miyakoshi and G. Cheng, "Examining human walking characteristics with a telescopic compass-like biped walker model," 2004 IEEE International Conference on Systems, Man and Cybernetics (IEEE Cat. No.04CH37583), The Hague, Netherlands, 2004, pp. 1538-1543 vol.2, doi: 10.1109/ICSMC.2004.1399850.

[4] Rummel J, Blum Y, Seyfarth A. Robust and efficient walking with spring-like legs. Bioinspir Biomim. 2010 Dec;5(4):046004. doi: 10.1088/1748-3182/5/4/046004. Epub 2010 Nov 15. PMID: 21079285.

[5] M. M. Pelit, J. Chang, R. Takano and M. Yamakita, "Bipedal Walking Based on Improved Spring Loaded Inverted Pendulum Model with Swing Leg (SLIP-SL)," 2020 IEEE/ASME International Conference on Advanced Intelligent Mechatronics (AIM), Boston, MA, USA, 2020, pp. 72-77, doi: 10.1109/AIM43001.2020.9158883.

[6] Tad McGeer, Passive Dynamic Walking, The International Journal of Robotics Research, Vol. 9, pp. 62-82, 1990, doi: 10.1177/027836499000900206.